Ultrasonics - Sonochemistry 56 (2019) 46–54

Contents lists available at ScienceDirect

Ultrasonics - Sonochemistry

journal homepage: www.elsevier.com/locate/ultson

A computational and experimental study on acoustic pressure for ultrasonically formed oil-in-water emulsion

T. Joyce Tiong[a,*], Jin Kiat Chu[a], Li Yan Lim[a], Khang Wei Tan[b], Yeow Hong Yap[c], Umi Aisah Asli[d]

[a] Department of Chemical and Environmental Engineering, University of Nottingham Malaysia, Jalan Broga, 43500 Semenyih, Selangor, Malaysia
[b] School of Energy and Chemical Engineering, Xiamen University Malaysia, 43900 Selangor, Malaysia
[c] Department of Chemical Engineering, Lee Kong Chian Faculty of Engineering and Science, Universiti Tunku Abdul Rahman, Sungai Long Campus, Jalan Sungai Long, Bandar Sungai Long, 43000 Kajang, Selangor, Malaysia
[d] Innovation Centre in Agritechnology for Advanced Bioprocessing, UTM Pagoh Research Center, Pagoh Educational Hub, 84600 Pagoh, Johor, Malaysia

ARTICLE INFO

Keywords:
COMSOL
Acoustics
Oil-in-water
Computational
Particle size
Experimental study

ABSTRACT

In the field of ultrasonic emulsification, the formation and cavitation collapse is one major factor contributing to the formation of micro- and nano-sized emulsion droplets. In this work, a series of experiments were conducted to examine the effects of varying the ultrasonic horn's position to the sizes of emulsion droplets formed, in an attempt to compare the influence of the simulated acoustic pressure fields to the experimental results. Results showed that the intensity of the acoustic pressure played a vital role in the formation of smaller emulsion droplets. Larger areas with acoustic pressure above the cavitation threshold in the water phase have resulted in the formation of smaller emulsion droplets *ca.* 250 nm and with polydispersity index of 0.2–0.3. Placing the ultrasonic horn at the oil-water interface has hindered the formation of small emulsion droplets, due to the transfer of energy to overcome the interfacial surface tension of oil and water, resulting in a slight reduction in the maximum acoustic pressure, as well as the total area with acoustic pressures above the cavitation threshold. This work has demonstrated the influence of the position of the ultrasonic horn in the oil and water system on the final emulsion droplets formed and can conclude the importance of generating acoustic pressure above the cavitation threshold to achieve small and stable oil-in-water emulsion.

1. Introduction

Ultrasound has been a common tool to use to form emulsion droplets due to its ability to shear the oil and water interface to form micro- and nano-sized, stable droplets [1]. It began to gain its popularity over the past few decades following to the success of Wood and Loomis in 1927 [2]. Ever since, scientists around the world have attempted to utilise this powerful tool to further enhance the properties of emulsion droplets formed and have thoroughly studied the fundamentals of this phenomena. Amongst the discoveries, Li and Fogler [3] were one of the pioneers who have elaborated on the theory of ultrasonic emulsification. They deduced that the emulsification process can be separated into a two-step mechanism. The first step involves the eruption of dispersed phase droplets into the continuous phase to form coarse emulsion; followed by the second step which involves intense cavitation collapse, resulting in disruption and mixing of the two phases to form very small, micro- to nano-sized droplets [4].

There have been many experimental based reports on the formation of ultrasonically assisted emulsion droplets. For example, Higgins and Skauen [5] have studied on the effects of hydrophilic-lipophilic balance (HLB), surfactants and ultrasonic power on the emulsion droplet sizes. Mujumdar et al. [6] have evaluated the effects of ultrasonic horn distance from the interface and irradiation time on the overall physicochemical properties of the emulsion droplets formed and found that the smallest emulsion droplet diameter can be achieved when the ultrasonic horn was placed 3 mm from the oil-water interface. Behrend and co-workers [7] reported a correlation between the hydrostatic pressure, energy density and the gas content that may affect the overall emulsion droplet sizes formed. Gaikwad and Pandit [8] studied that the physicochemical properties of the dispersed phase (oil phase) and have concluded that the viscosity of the dispersed phase have great impact in the overall formation of emulsion droplets. Apart from the formation of emulsion, ultrasound was also used to form double emulsion droplets [9], to separate emulsion droplets [10], to remove arsenic impurities *via* ultrasonically formed emulsification [11], and even to demulsify oil-in-water (O/W) emulsions by the application of ultrasonic standing

* Corresponding author.
E-mail address: joyce.tiong@nottingham.edu.my (T.J. Tiong).

https://doi.org/10.1016/j.ultsonch.2019.03.026
Received 28 June 2018; Received in revised form 19 March 2019; Accepted 26 March 2019
Available online 27 March 2019
1350-4177/

Nomenclature

α	Attenuation coefficient (m^{-1})	L_{oil}	Height of oil layer from oil-air interface (cm)
ρ	Density of the liquid medium ($kg\,m^{-3}$)	m	Mass of water in the system (kg)
ω	Angular frequency ($rad\,s^{-1}$)	P_{out}	Total power output (W)
A	Cross-sectional area of the ultrasonic horn (m^2)	p_o	Acoustic pressure amplitude (Pa)
C_p	Specific heat capacity of water ($J\,kg^{-1}\,°C^{-1}$)	p	Acoustic pressure (Pa)
c	Speed of sound in liquid medium (m/s)	r	Spatial variable, $r = [x, y, z]$
I	Ultrasonic intensity ($W\,m^{-2}$)	ΔT	Difference in temperature (°C)
L	Length of immersion of ultrasonic horn (cm)	Δt	Difference in time (s)
		W	Width of the vessel (cm)
		x_i	Point coordinate (m)

waves [12].

Among the many applications of ultrasound in the field of emulsification, it is of common knowledge that cavitation plays an important role in both the emulsification and de-emulsification processes. The formation and eventual collapse of cavitation bubbles depend on various parameters, varying from the viscosity of the fluid, gas content, ultrasonic power density, solution temperature, and so on [13]. Among these parameters, acoustic pressure plays an important role in the formation of transient cavitation, where the acoustic pressure applied to the system has to reach a certain minimum (termed cavitation threshold) to shear the liquid molecules apart to form cavities [14]. Owing to the importance of the acoustic pressure in ultrasonic systems, many have ventured into performing simulation studies on the acoustic pressure fields in their respective systems. For example, Saez et al. [15] and Klima et al. [16] showed successful correlation of acoustic pressure simulation to the experimental data, where areas simulated with high acoustic pressure showed the greatest cavitation activity in their experiments. Following to that, Tiong et al. [17] and Price et al. [18] have also employed simulation techniques to determine the factors affecting the acoustic pressure generated for a dental equipment, whilst Wei and Weavers [19] have employed similar technique to optimise the design of their sonoreactor. Sajjadi and co-workers [20] correlated their computational fluid dynamics (CFD) results to experimental data from particle image velocimetry, whilst Zhang et al. [21] validated their fluid-structure interaction harmonic response study *via* an aluminium foil erosion test. A recent study on the measurement of sound field in a sonochemical reactor by Yasuda et al. [22] have revealed in their simulation results that the areas with high sound pressures may result in weaker reaction fields. On the other hand, others have investigated the numerical acoustic pressure fields upon the application of a single frequency [23] and multifrequency ultrasound [24] in their systems.

Other key factors affecting the quality of the resulting emulsion includes the generation of bulk fluid flows which facilitates macromixing between the oil and water phases. In acoustic systems, these bulk flows are generated from through acoustic streaming, where fluid flow is driven by the acoustic pressure driving force. Kojima et al. [25] experimentally studied the effect of acoustic power on acoustic streaming and sonochemical efficiency in a reactor. Similarly, studies conducted by Xu and co-workers [26,27] have provided valuable insight on acoustic streaming phenomena through a series of computational studies.

Further to that, some researchers have attempted to couple multiple physics onto their simulation studies. For example, Niazi and co-workers [28] have performed simulation studies on the acoustic pressure distribution and the thermodynamic conditions in a sonoreactor designed for the upgrading of crude oil. Whilst others performed multiphysics simulations by coupling the acoustic field, chemical kinetics, reactive flow and cavitation attenuation to investigate the feasibility of a sonoreactor for transesterification [29]. Recently, a study published by Tian et al. [30] reported the use of a 3D finite element model to study the effect of acoustic pressure distribution on the cavitation erosion of ultrasonic sonotrodes in large-scale, ultrasound-assisted casting systems. Some other researchers have attempted to incorporate the cavitation phenomena to the acoustic pressure field, such as the employment of Eulerian two-fluid approach [31], solving of non-linear acoustic wave with bubble dynamics [32–34], study on the effects of bubble clouds upon subjected to ultrasonic waves [35], attempt to simulate the surface cleaning by cavitation bubbles [36], study on the effects of varying static pressure to the bubble dynamics [37] and an evaluation on the interaction between cavitation bubble and biological cells [38].

Despite numerous efforts in performing various simulation of acoustic pressure fields for the correlation and optimisation of different ultrasonic systems, to date, there is still a lack of reports in the acoustic simulation of a two-phase liquid system. Most of the reports on multiphase ultrasonic systems focused on the separation of oil-in-water (O/W) or water-in-oil (W/O) emulsions. For example, Hou et al. [39] have attempted to simulate the vibration and propagation of ultrasonic wave in a multiphase system for the oil recovery technology. Wang et al. [40] attempted to simulate the phase separation of oil-in-water emulsion in ultrasound field by employing the lattice Boltzmann method. On the other hand, Pedrotti et al. [41] have recently reported a correlation of acoustic pressure intensity in an ultrasonic bath to the effectiveness of separating W/O emulsion droplets. However, there is still no report on the correlation of acoustic pressure fields in a two-phase system and how it may eventually affect the properties of the emulsion droplets formed. Seeing the research gap, this paper aims to evaluate the effects of the simulated acoustic pressure fields in a two-phase oil and water system, to correlate the simulated results to the experimental findings in the formation of O/W emulsion.

2. Methodology

2.1. Acoustic pressure simulation

Calorimetric method was used to determine the actual power dissipated and energy efficiencies of the equipment. The experiment was carried out by measuring the temperature rise over a period of 10 min without running cooling water around the system, under sonication amplitude of 50%, taking the temperature readings every 30 s. The total power output was calculated using Eq. (1),

$$P_{out} = \frac{mC_p\Delta T}{\Delta t} \tag{1}$$

where P_{out} is the power dissipated (W); m is the mass of water (kg); C_p is the specific heat capacity of water ($J\,kg^{-1}\,°C^{-1}$); ΔT is the change in temperature (°C); while Δt is the change in time (s). For the experiment, 200 mL of distilled water was used in a 250 mL beaker.

The ultrasonic system used in this work was a 23 kHz ultrasonic probe with a probe diameter of *ca.* 1 cm. The probe was inserted into the beaker of water at a fixed height with 1 cm for the experiments conducted to determine the power dissipation into the system. Subsequent changes in the height of the ultrasonic probe was varied at 0.5, 1.5 and 2 cm from the air-water interface to examine the effects of ultrasonic probe position to the power dissipated into the system (See Fig. 1).

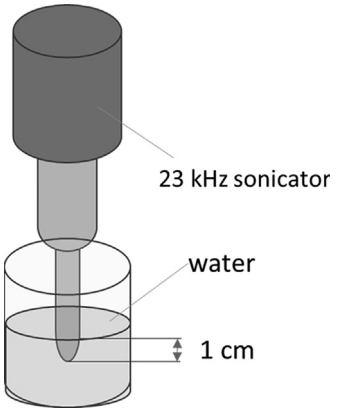

Fig. 1. Schematic showing the position of the sonicator immersed in the liquid at a fixed height of 1 cm from the liquid interface.

The active zones in an ultrasonic system are highly dependent on the acoustic pressure. Simulations were performed using the pressure acoustics frequency domain in COMSOL Multiphysics 5.2 using finite element method (FEM), which encompasses the solving of complex engineering problems like acoustic propagations governed by partial differential equations (PDEs) [19].

Intensity, I of the system was obtained based on Eq. (2),

$$I = \frac{P_{out}}{A} \tag{2}$$

where P_{out} is the total power dissipated into the system, obtained experimentally through calorimetry; and A is the cross-sectional area of the ultrasonic horn, calculated to be around $8 \times 10^{-5}\,m^2$.

From there, the acoustic pressure amplitude, $p_o(r)$, can be obtained based on Eq. (3) below.

$$I(r) = \frac{p_o^2(r)}{2\rho c} \tag{3}$$

Which will subsequently give,

$$p_o(r) = \sqrt{\frac{2\rho c P_{out}}{A}} \tag{4}$$

where r is the spatial variable (r = [x, y, z]), ρ is the density of the medium (kg m^{-3}) and c is the sound velocity in the medium (m s^{-1}).

The acoustic pressure simulation for the ultrasonic system was performed based on a method described by Tiong et al. [42] by applying the simplified Helmholtz equation in Eq. (5).

$$\nabla\left(-\frac{1}{\rho}\nabla p\right) - \frac{\omega^2}{\rho c^2} p = 0 \tag{5}$$

where ω is the angular frequency (rad s^{-1}); p is the acoustic pressure (Pa).

The mesh generated for FEM of this study was a predefined tetrahedral mesh, validated by increasing the numbers of degree of freedoms until a negligible effect was obtained, to decrease the pollution effect in the model [43]. This results in a final amount of 54,405 number of degrees of freedoms for a 2D axisymmetric simulation. Fig. 2 illustrates (a) the dimensions and notations used to define the variables in simulation and (b) the mesh generated for the simulation process. To initiate the simulation on acoustic pressure, the first correlation was performed to look at the effects of the depth of the ultrasonic horn, L, to the overall acoustic pressure.

The simulation was conducted using a fixed dimension to emulate the dimensions of a 250 mL beaker, with width, W of 6.5 cm and overall liquid height of 6 cm, unless stated otherwise.

Below are the boundary conditions and simulation parameters used.

(i) Air-water interface: simulated as sound soft boundary, indicating that there is a total reflectance of sound wave upon approaching the interface, resulting in acoustic pressure, $p = 0$ at the interface.
(ii) Walls of the ultrasonic tip: Acoustic impedance of titanium, corresponding to 28.5 MRayl [44], which will result in sound reflectance and transmittance to occur based on the properties of the material.
(iii) Walls of the vessel: simulated based on the acoustic impedance of a borosilicate glass [45], corresponding to 13 MRayl [46], which will result in sound reflectance and transmittance to occur based on the properties of the material.

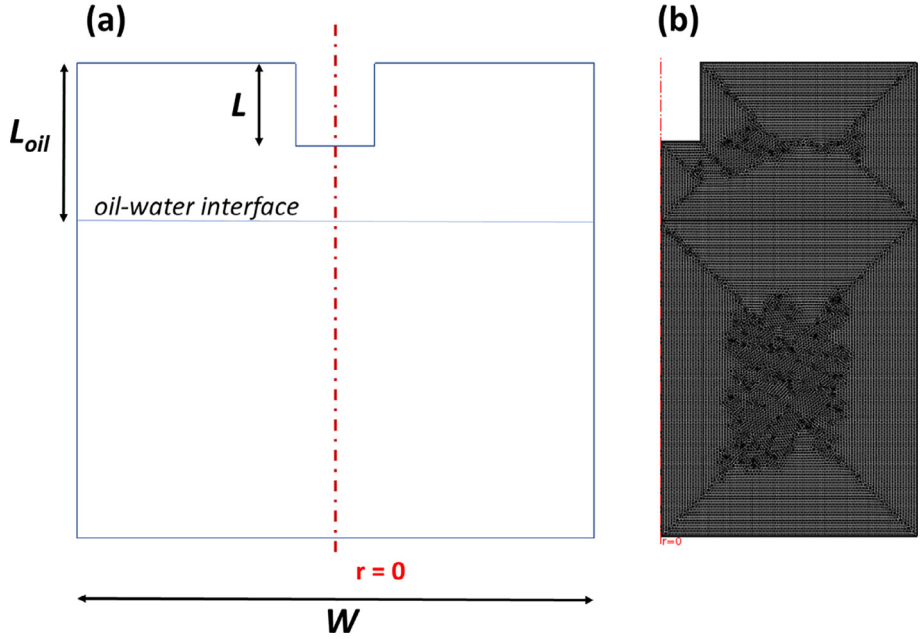

Fig. 2. (a) Notations used to describe the various dimensions used for the simulation process. L_{oil}: height of oil from the air-oil interface; L: length of immersion of the ultrasonic horn and W: width of the vessel (all in cm); (b) Mesh generated for acoustic simulation.

(iv) The entire vessel consists of either 1 or 2 domains.
   a. For single phase system when only water is present, the domain is water, using predefined physical properties provided in the software.
   b. For two phase systems, the upper domain at the upper vessel is simulated as oil, carrying density of 930 kg m^{-3} and speed of sound of 1456 m s^{-1} [47].

(v) The linear acoustics model employed for this simulation study which will consider of the attenuation based on the material properties and boundary conditions stated.

2.2. Experimental validation

A series of experiments were conducted to validate the simulation works performed, as described below.

2.2.1. Preparation of oil-in-water emulsion

The oil used in this experiment was palm oil based (Helang, Yee Lee Edible Oils Sdn. Bhd., Malaysia). Deionised water (Milli-Q®, Merck, 18.2 MΩ) was used throughout the entire experiment. Sonication of the oil-in-water emulsion was performed using a 23 kHz Sonics and Materials ultrasonic probe (VCX 750, 750 W), with a probe diameter of *ca.* 1 cm. The oil and water mixture were placed carefully in a 250 mL (I. D. = 6.5 cm) beaker, with 4 cm in height of water and 2 cm of oil, corresponding to a total of 200 mL of oil and water mixture.

2.2.2. Video recording

To examine the extent of cavitation in an oil and water mixture, a series of videos were captured using a digital single lens reflex camera (dSLR, Nikon D5100), mounted to a Nikon zoom lens (AF-S Nikkor 18–105 mm, F3.5–5.6). The conditions of the video capturing were set to be constant at 30 fps, ISO 500, F3.5 and at a magnification distance of 70 mm. The camera was placed at a fixed distance of 40 cm away from the beaker, and the videos were captured continuously over a sonication duration of 1 min, as shown in Fig. 3. The experiments were conducted by varying the position of the ultrasonic probe height, *L*, ranging from 0.5, 1.0, 1.5, 1.9 and 2.0 cm from the air-oil interface. The results were extracted frame-by-frame using an in-built video editing software (iMovie, iOS 11, Apple Inc.) and the extent of the cavitation taken place were analysed using ImageJ.

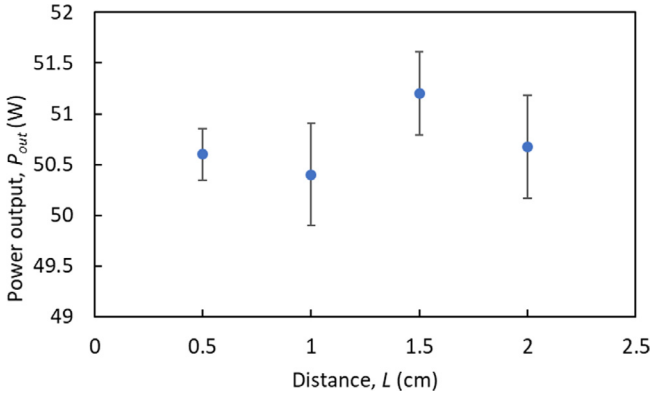

Fig. 4. Power dissipated into the system at various ultrasonic horn length.

2.2.3. Particle size analysis

The mean droplet size and size distribution of O/W emulsion was determined by means of dynamic light scattering using Zetasizer Nano-ZS (Malvern Instruments, United Kingdom) and the Zetasizer® software (version 7.03). Each analysis was carried out at a fixed scattering angle of 173° at 25 °C and was presented with three independent measurements, which comprised of five acquisitions each. For each experimental condition, three independent samples were analysed and the average value of Z-average and polydispersity index (PDI) was presented.

3. Results and discussion

3.1. Effects of ultrasonic horn position to the acoustic pressure

The acoustic pressure computational study was initiated by determining the power dissipated into the system. This was achieved by performing calorimetry at various ultrasonic horn positions, with results illustrated in Fig. 4. From Fig. 4, the power dissipated into the system can be seen to have slight variations upon varying the height of the ultrasonic horn from the air-water interface. However, these differences are insignificant (P-value > 0.05), and therefore an average power output of 50.7 W, corresponding to 1.389 MPa was used for all subsequent acoustic simulations.

Acoustic pressure simulation of the ultrasonic horn at various horn

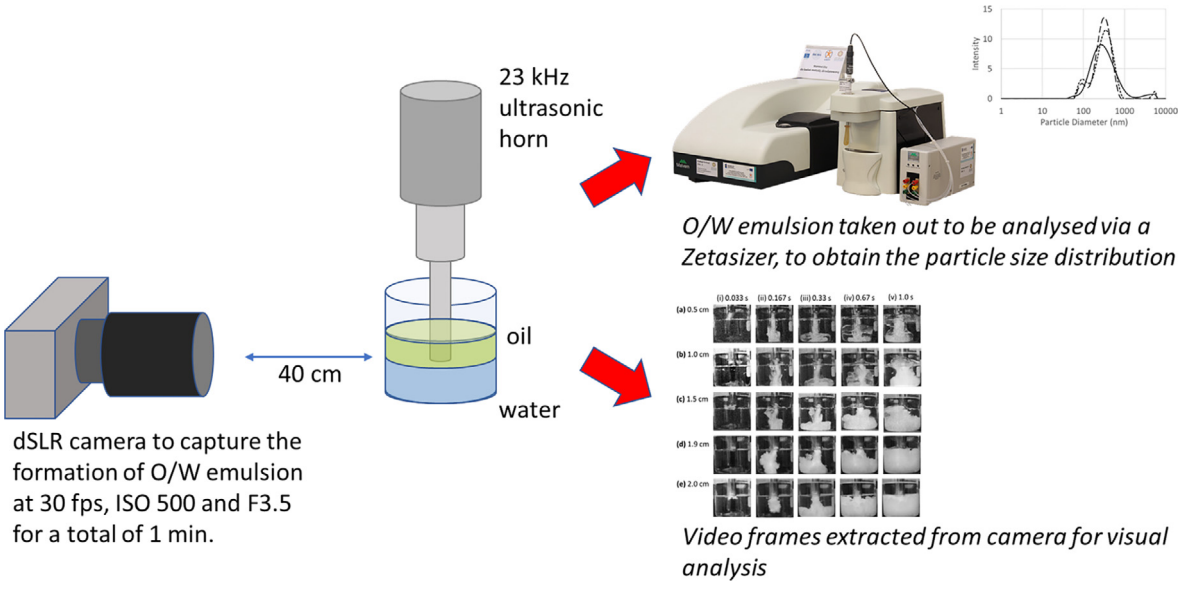

Fig. 3. Schematic of the experimental setup for the video recording and the particle size analyses for the O/W emulsification process.

height was first simulated in a single-phase water system, as illustrated in Fig. 5. The results collated showed that the position of the ultrasonic horn, had showed significant effects on the acoustic pressure fields. With reference to Fig. 5(a)–(e), it can be seen that the maximum absolute acoustic pressures (Abs. P_{max}), were the greatest when the ultrasonic horn was closer to the air-water interface, amounting to approximately 1 MPa when the ultrasound was 0.5 and 1.0 cm away from the air-water interface. There is a decreasing trend in the Abs. P_{max} upon further immersion of the ultrasonic horn in the water system. The sound wave generated by the ultrasonic horn propagates from the tip of the horn. The large impedance difference between water and air causes total reflectance of propagating sound waves back into the water. Therefore, when the position of the ultrasonic horn is closer to the air-water interface, this results in a higher level of reflectance in sound wave, hence generating slightly higher maximum acoustic pressures [48]. On the other hand, when the ultrasonic horn tip is positioned lower or further away from the air-water interface, lower magnitudes in sound reflectance are created due to a certain degree of sound attenuation, therefore resulting in lower maximum acoustic pressure.

Despite generating the highest maximum acoustic pressure when the ultrasonic horn was close to the air-water interface, it should be noted that the production of cavitation and sonochemical activities will only occur when the cavitation threshold pressure is achieved. With reference to Fig. 5(a), despite generating the highest absolute acoustic pressure, the main body of the simulated area merely showed regions with acoustic pressures of < 0.5 MPa, suggesting weaker cavitation activities when it is further down in the beaker, as compared to the other positions in Fig. 5(b)–(e). This resonates with the report by Mujumdar et al. [6], where they have showed that higher potassium iodine was deliberated when the ultrasonic horn was placed deeper down in the water, which may be contributed to wider regions of acoustic pressures above the cavitation threshold. It was also reported that the maximum acoustic pressure that can be achieved in the system was strongly related to the resonance length between the ultrasonic source to the overall size of the tank [23]. In this work, the simulated frequency was 23 kHz, which corresponds to a sound wavelength of *ca.* 6.5 cm in water. When the ultrasonic horn tip was placed at 0.5 cm from the air-water interface, this corresponded it to be closer to the resonating wavelength of the ultrasonic system, hence generating higher maximum acoustic pressure near the ultrasonic horn tip. Another contributing factor of the reduction of acoustic pressure generated when $L = 0.5$ cm was to do with the attenuation of sound. The literature reported an attenuation of 40% at 50 mm away from the ultrasonic source, at comparable ultrasonic intensities and frequency of 0.25 W cm^{-3} at 24 kHz [49]. This gave rise to a significant attenuation at the water system when the ultrasonic source was placed further away from the oil-water interface, resulting in lower acoustic pressures.

3.2. Effects of length of ultrasonic horn, L in L_{oil} to the acoustic pressure

Fig. 6 illustrates the acoustic pressure fields at different ultrasonic horn lengths in an oil and water system. It can be noted that the overall acoustic pressure fields were similar to those of only water (Fig. 5), but with slight difference in the Abs. P_{max}. With reference to Fig. 6(a)–(d), placing the ultrasonic horn in the oil phase have slightly increased the maximum acoustic pressures by approximately 2–5 kPa. Based on Eq. (5), when the initial pressure supplied to the system remains the same, submersing the ultrasonic horn in the oil phase, which has lower density and speed of sound as compared to water, will result in an increase in the acoustic pressure generated in the system.

Despite having only slight changes in the Abs. P_{max} generated in both water and oil-water systems, it is interesting to note that placing the ultrasonic horn right at the oil-water interface, as shown in Fig. 6(e), has attenuated the acoustic pressure generated. This could be contributed to the transfer of energy to overcome the interfacial tension between the oil and water at the interface [6], resulting in a reduction in acoustic pressure generated. The formation of oil-in-water emulsion *via* sonication is highly influenced by the formation of transient cavitation, which is highly dependent on the acoustic pressure generated. The cavitation threshold is different in oil and water, with an estimated cavitation threshold to be *ca.* 1–1.5 MPa in oil [50] and 0.5 MPa in water [51]. Therefore, based on the simulated acoustic pressure fields, it can be concluded that whilst placing the ultrasonic horn higher up the beaker will generate a higher Abs. P_{max}, it is also important factor to ensure that the acoustic pressure generated in the water system is higher than the cavitation threshold, in order to ensure that cavitation occurs at majority of the areas in the system.

One factor contributing to the formation of ultrasonically induced O/W emulsion is the formation of cavitation in the water, resulting in micro oil droplets to be encapsulated in the water system. Table 1 compares of areas with > 0.5 MPa for in the water at different horn lengths, calculated with the aid of ImageJ. There, it can be seen that placing the horn too high up in the oil-phase may result in the absence of acoustic pressure field beyond the cavitation threshold in the water phase. Hence, despite being able to generate high maximum acoustic pressure in the oil phase (as shown in Fig. 6), the absence of substantial acoustic pressure in the water may be one contributing factor to the formation of coarser O/W emulsion droplets. Further, comparing the lengths of 1.9 and 2.0 cm, it can be noted that there was a significant suppression in the acoustic pressure when the horn was placed at the oil-water interface, forming a relatively lower area with acoustic pressure > 0.5 MPa.

Mujumdar et al. [6] showed that the distance between the ultrasonic tip and the oil-water interface had significant effects in the diameter of the O/W emulsion droplets. In their experimental work, they showed that placing the ultrasonic horn close to the oil-water interface gave the best results in terms of O/W emulsion with the smallest

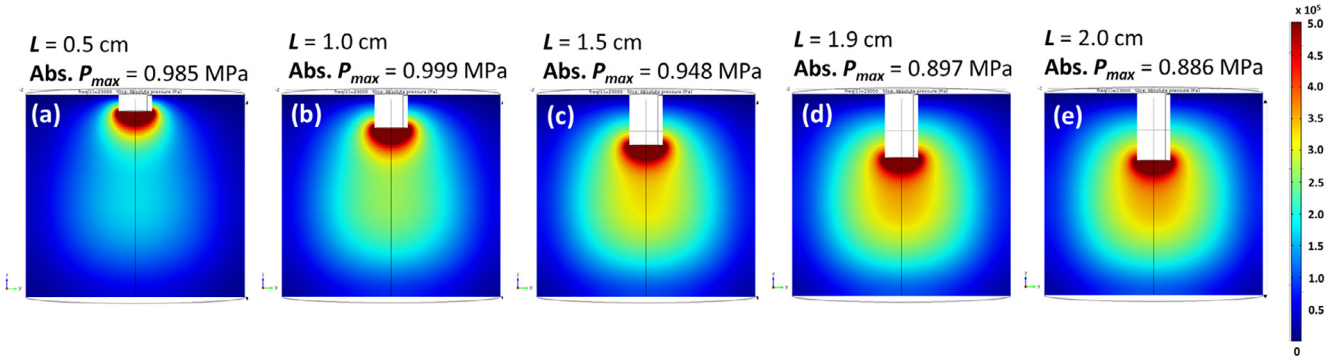

Fig. 5. Absolute acoustic pressure fields (Pa) obtained upon subjected to sonication in water at initial acoustic pressure of 1.389×10^6 Pa at varying ultrasonic horn lengths of (a) 0.5 cm; (b) 1.0 cm, (c) 1.5 cm, (d) 1.9 cm and (e) 2.0 cm.

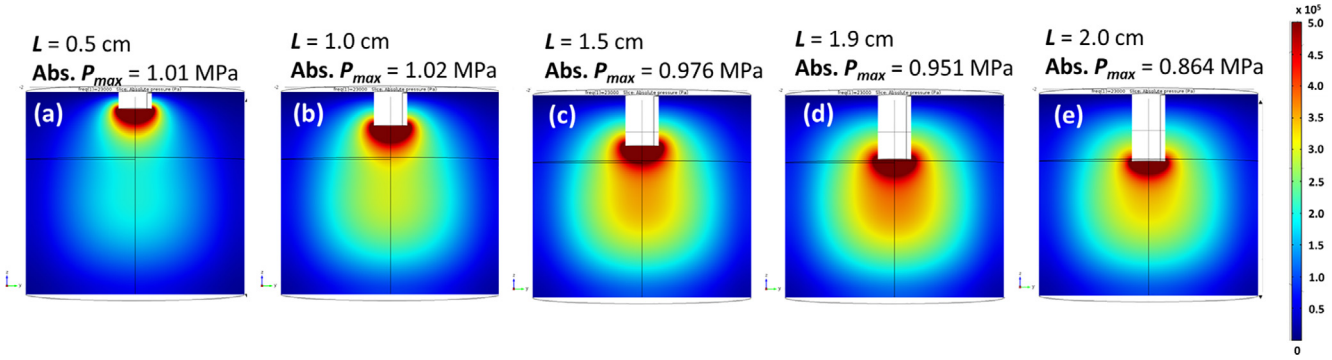

Fig. 6. Absolute acoustic pressure (Pa) obtained upon subjected to sonication in oil (L_{oil} = 2 cm) and water at initial acoustic pressure of 1.389 × 10^6 Pa at varying ultrasonic horn lengths of (a) 0.5 cm; (b) 1.0 cm, (c) 1.5 cm, (d) 1.9 cm and (e) 2.0 cm.

Table 1
Area with > 0.5 MPa at various ultrasonic horn length immersed in the oil and water system.

Length, *L* (cm)	Area with > 0.5 MPa in the water phase (arbitrary unit, a. u.)
0.5	0
1.0	0
1.5	439
1.9	4304
2.0	3231

particle diameter and higher stability emulsion droplets. With reference to the simulation results obtained in Figs. 5 and 6, it can be seen that there is a correlation in this work as compared to the literature [6], where the area with high acoustic pressure is greater when the ultrasonic horn was placed closer to the oil-water interface, which will subsequently contribute to higher cavitation activity.

3.3. Videos of the formation of O/W emulsion at different L

Experiments of the formation of O/W emulsion with a fixed L_{oil} at varying depth of the ultrasonic horn, *L*, were performed and compared to the simulated results. Fig. 7 collates the screenshots of the O/W emulsion formed at varying time intervals. Here, the frames collated can roughly be separated into two categories: the first will be for *L* of 0.5 and 1.0 cm (Fig. 7(a) and (b)), while the second category for *L* of 1.5, 1.9 and 2.0 cm (Fig. 7(c)–(e)). For the first group, the cavitation and acoustic streaming process was focused along the middle of the vessel. Even after sonication of 1 s, the water interface was still not entirely blanketed by the oil phase. Whereas, in the second group, it can generally be seen that the cavitation and acoustic streaming activity have resulted in vigorous mixing of the oil and water system, resulting in almost 100% coverage of oil in water after sonication of 1 s. This shows that there is a close correlation of the O/W emulsion to the position of the ultrasonic source.

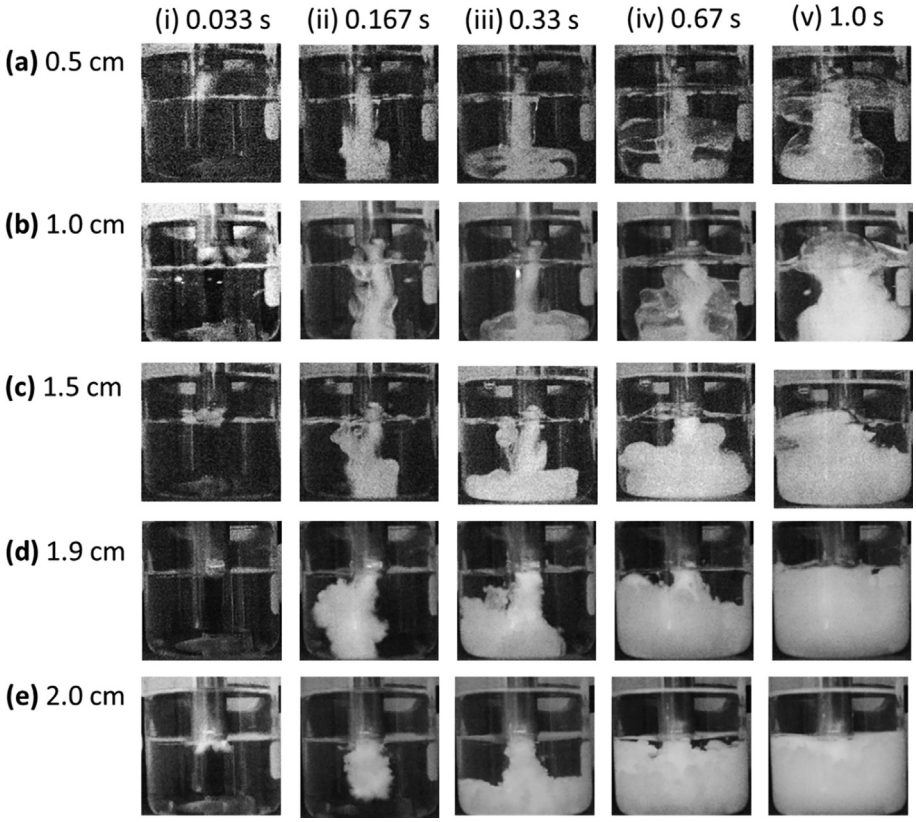

Fig. 7. Formation of O/W emulsion at varying depth of the ultrasonic horn, L, at different time intervals.

To further evaluate the performance of the O/W emulsion formed, Fig. 8 collates the total area of the emulsion 'cloud' for the first 5 frames of the video with the aid of ImageJ. At time < 0.1 s, the formation of emulsion 'cloud', containing a mixture of cavitation and results of acoustic streaming in the system, was insignificant across different depth of the ultrasonic horn. However, upon reaching the 0.1 s mark, there was a distinctive difference between *L* of 1.5 and 1.9 cm, as compared to the others, where they have managed to form large areas of emulsion cloud in the water phase.

The reduced intensity of cavitation cloud and streaming activity for 0.5 and 1.0 cm in Fig. 7 can be strongly related to the higher cavitation threshold in oil. As shown in Fig. 6, the estimated acoustic cavitation pressure in oil is *ca.* 1 MPa, which is approximately 2 times higher than water. Therefore, placing the ultrasonic horn in the middle of the oil phase will affect the formation of cavitation bubbles, since most of the oil phase is below its cavitation threshold, which will eventually affect the quality of the O/W emulsion formed. On the other hand, when the ultrasonic horn is positioned closer to the oil-water interface, substantial acoustic pressure above the cavitation threshold will be generated in the water phase, therefore forming pockets of oil-filled bubbles – hence forming O/W emulsion droplets.

The results obtained in Fig. 8 has also correlated well with the simulated acoustic pressure (Fig. 6), where there was a general trend of lower spread of high acoustic pressure regions when the depth of the ultrasonic horn was 0.5 and 1 cm. Apart from that, it can also be seen that when the ultrasonic source was placed exactly at the oil-water interface, in Fig. 7(e) (ii), there was a distinctive reduction in total area of emulsion cloud formation, as compared to *L* of 1.5 and 1.9 cm. As the ultrasonic energy supplied to the system was used up to overcome the interfacial tension of the oil-water interface, causing a reduction in the spread of O/W emulsion clouds formed in the beginning of the emulsification process, at $t = 0.0033$ s in Fig. 7. The formation of O/W emulsion *via* sonication is highly dependent on formation of transient cavitation, which is responsible to shear the interfacial force between the oil-water interface to form small emulsion droplets [52]. Placing the ultrasonic horn close to the oil-water interface will benefit the production of high acoustic pressures, which will increase the tendency of transient cavitation production, hence producing more O/W emulsion droplets. When the ultrasonic horn is placed at the oil-water interface, the presence of interfacial tension between oil and water will result in the production of a radiation pressure called Rayleigh pressure [53]. Therefore, high fluid particle velocity is required to overcome the Rayleigh pressure at the interface, before transforming its energy to produce cavitation bubbles.

3.4. O/W particle size analysis

Further analysis on the emulsion droplets formed was performed on a Zetasizer to determine the average particle sizes and their distribution. Results obtained in Fig. 9 shows a distinctive difference in particle sizes when the horn was at *L* of 0.5, 1, and 2 cm, with particle sizes > 400 nm and with polydispersity index (PDI) of 0.4–0.5, as compared to the other horn position of 1.5 and 1.9 cm, which had much smaller particle sizes in the range of 250 nm and with PDI of 0.2–0.3. Here, a strong correlation between the areas with high acoustic pressure fields in the water phase is highly responsible in the formation of stable and smaller O/W emulsion droplets, which is again attributed to the formation of transient cavitation bubbles under those conditions.

The power supplied to the system, which can be correlated to the acoustic pressure generated in the system, plays an important role in the formation of O/W emulsion. Ramisetty and co-workers [54] have previously reported that higher power supply has resulted in O/W emulsion with smaller sizes. Since the power supplied to the system will affect the overall acoustic pressure generated, therefore the influencing the O/W emulsion sizes. Apart from that, the ultrasonic frequency also plays a role in contributing to the O/W emulsion droplet sizes. Supplying higher frequency of ultrasound will result in the formation of smaller cavitation, which will eventually form smaller oil droplets [55]. However, it must be noted that this is also highly dependent on the power supplied to the system, as the cavitation threshold increases with the ultrasound frequency [55]. Therefore, it was concluded that the ideal frequencies to conduct ultrasonic emulsification effectively still lies in the ranges of 20–40 kHz [56], to achieve the desired dispersion of ultrasonic energy to form stable emulsion droplets.

Li and Fogler [4] have mentioned that the formation of submicronic emulsions involves two mechanisms: first was to erupt the dispersed phase into the continuous phase; followed by further cavitation disruption and mixing into smaller droplet sizes. Therefore, it is important to have zones with high acoustic pressure near the oil-water interface to have substantial energy to erupt the interface and allowing the dispersed phase (ie. oil) to enter the continuous phase (ie. water), as well as acoustic pressure zones above the cavitation threshold in the continuous phase, to further disrupt the oil molecules into smaller O/W emulsion. This explains the importance of the placement of the ultrasonic horn to be at an optimum position which will create sufficient acoustic pressure in both the oil and water phases, to produce smaller and hence more stable emulsion droplets.

There were several studies in the literature on the effects of ultrasonic horn or bath position to the overall emulsion droplet sizes and stability [6,57]. Kojima and co-workers [57] found out that there was an optimum distance of the ultrasonic source from the bottom of the vessel to produce emulsion with the highest stability. Similarly, this work showed that ultrasonic horn depth placement of 1.5–1.9 cm has resulted in emulsions with significantly lower average particle sizes, and with lower polydispersity, as shown with the error bars in Fig. 9. Therefore, this concludes that the position of the ultrasonic horn and the acoustic pressure generated in the oil and water system hold important roles in the formation of stable, ultrasonically formed O/W emulsion droplets.

4. Conclusion

This work has successfully correlated the effects of ultrasonic horn position to the acoustic pressure generated, which have affected the formation of O/W emulsion droplets. Acoustic pressure simulation showed that the maximum acoustic pressure generated reduces with the increase in ultrasonic horn depth into the liquid system, but the overall area with high acoustic pressure region showed reverse phenomena. Placing the ultrasonic horn closer to the oil-water interface had generally resulted in the production of larger areas with acoustic pressures above the cavitation threshold. Experimental validation showed that the acoustic pressure generated above cavitation threshold played an important role to form emulsion droplets. Ultrasonic horn placed closer

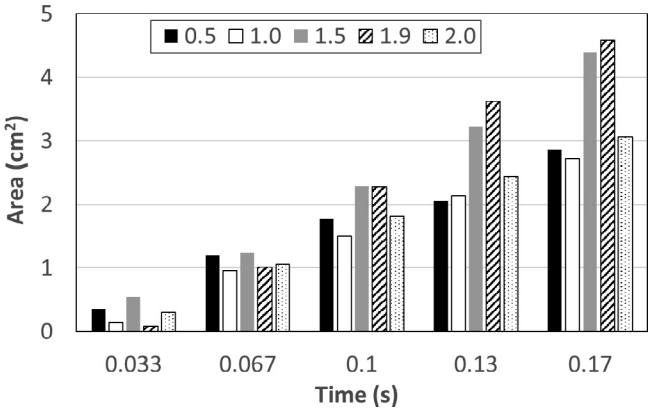

Fig. 8. Area of emulsion 'cloud' formed at different depth of the ultrasonic horn, L, in the system, at varying time intervals.

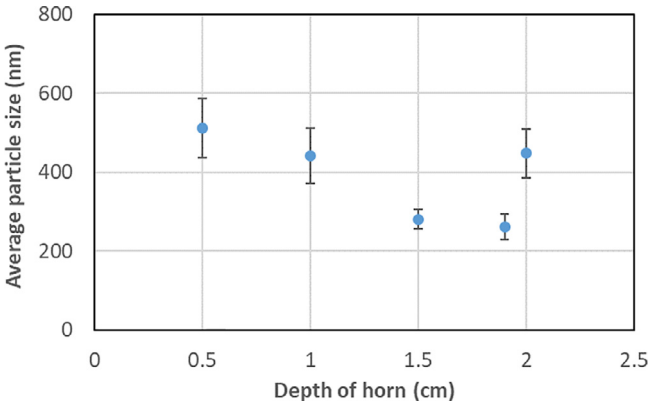

Fig. 9. Average particle sizes of the O/W emulsion formed upon sonication for 1 min at varying depth of the ultrasonic horn, L.

to the oil-water interface (at L = 1.5 and 1.9 cm) resulted in the production of smaller emulsion droplets of diameters *ca.* 250 nm, and PDI of 0.2–0.3, whilst placing right at the oil-water interface showed adverse effect, due to the transformation of ultrasonic energy to overcome the interfacial surface tension and radiation pressure at the interface. Therefore, this work concludes that the acoustic pressure generated in both the oil and water phases possess significant effects in the final production of stable O/W emulsion droplets.

Acknowledgements

The authors are grateful to receive funding from the Ministry of Higher Education (MoHE), Malaysia *via* Fundamental Research Grant Scheme (FRGS/2/2014/TK05/UNIM/02/1) for this work.

References

[1] S.M. Jafari, Y. He, B. Bhandari, Nano-emulsion production by sonication and microfluidization – a comparison, Int. J. Food Prop. 9 (3) (2006) 475–485.
[2] Wood, R. W. and Loomis, A. L. (1927) XXXVIII. The physical and biological effects of high-frequency sound-waves of great intensity, The London, Edinburgh, and Dublin Philosophical Magazine and Journal of Science, 4(22), pp. 417–436.
[3] M.K. Li, H.S. Fogler, Acoustic emulsification. Part 1. The instability of the oil-water interface to form the initial droplets, J. Fluid Mech. 88 (3) (1978) 499–511.
[4] M.K. Li, H.S. Fogler, Acoustic emulsification. Part 2. Breakup of the large primary oil droplets in a water medium, J. Fluid Mech. 88 (3) (1978) 513–528.
[5] D.M. Higgins, D.M. Skauen, Influence of power on quality of emulsions prepared by ultrasound, J. Pharm. Sci. 61 (10) (1972) 1567–1570.
[6] S. Mujumdar, P. Senthil Kumar, A.B. Pandit, Emulsification by ultrasound: relation between intensity and emulsion quality, Indian J. Chem. Technol. 4 (1997) 277–284.
[7] O. Behrend, K. Ax, H. Schubert, Influence of continuous phase viscosity on emulsification by ultrasound, Ultrason. Sonochem. 7 (2) (2000) 77–85.
[8] S.G. Gaikwad, A.B. Pandit, Ultrasound emulsification: effect of ultrasonic physicochemical properties on dispersed phase volume and droplet size, Ultrason. Sonochem. 15 (2008) 554–563.
[9] T.S.H. Leong, M. Zhou, N. Kukan, M. Ashokkumar, G.J.O. Martin, Preparation of water-in-oil-in-water emulsions by low frequency ultrasound using skim milk and sunflower oil, Food Hydrocolloids 63 (2017) 685–695.
[10] F.G. Antes, L.O. Diehl, J.S.F. Pereira, R.C.L. Guimarães, R.A. Guanieri, B.M.S. Ferreira, V.L. Dressler, E.M.M. Flores, Feasibility of low frequency ultrasound for water removal from crude oil emulsions, Ultrason. Sonochem. 25 (2015) 70–75.
[11] S. Kiani, S.M. Mousavi, Ultrasound assisted preparation of water in oil emulsions and their application in arsenic (V) removal from water in an emulsion liquid membrane process, Ultrason. Sonochem. 20 (2013) 373–377.
[12] H. Ghafourian Nasiri, M.T. Hamed Mosavian, R. Kadkhodaee, Demulsification of gas oil/water emulsion via high-intensity ultrasonic standing wave, J. Dispersion Sci. Technol. 34 (4) (2013) 483–489.
[13] Y.T. Shah, A.B. Pandit, V.S. Moholkar, Factors affecting cavitation behaviour, Cavitation Reaction Engineering. The Plenum Chemical Engineering Series, Springer, Boston, MA, 1999.
[14] L.A. Crum, Acoustic cavitation thresholds in water, in: W. Lauterborn (Ed.), Cavitation and Inhomogeneities in Underwater Acoustics. Springer Series in Electrophysics, Springer, Berlin, Heidelberg, 1980.
[15] V. Saez, A. Frias-Ferrer, J. Iniesta, J. Gonzalez-Garcia, A. Aldaz, E. Riera, Characterization of a 20 kHz sonoreactor. Part 1: analysis of mechanical effects by classical and numerical methods, Ultrason. Sonochem. 12 (2005) 59–65.
[16] J. Klima, A. Frias-Ferrer, J. Gonzalez-Garcia, J. Ludvik, V. Saez, J. Iniesta, Optimisation of 20 kHz sonoreactor geometry on the basis of numerical simulation of local ultrasonic intensity and qualitative comparison with experimental results, Ultrason. Sonochem. 14 (2007) 19–28.
[17] T.J. Tiong, G.J. Price, S. Kanagasingam, A computational simulation study on the acoustic pressure generated by a dental endosonic file: effects of intensity, file shape and volume, Ultrason. Sonochem. 21 (5) (2014) 1858–1865.
[18] G.J. Price, T.J. Tiong, D.C. King, Sonochemical characterisation of ultrasonic dental descalers, Ultrason. Sonochem. 21 (6) (2014) 2052–2060.
[19] Z. Wei, L.K. Weavers, Combining COMSOL modelling with acoustic pressure maps to design sono-reactors, Ultrason. Sonochem. 31 (2016) 490–498.
[20] B. Sajjadi, A.A.A. Raman, S. Ibrahim, Influence of ultrasound power on acoustic streaming and micro-bubbles formations in a low frequency sono-reactor: mathematical and 3D computational simulation, Ultrason. Sonochem. 24 (2015) 193–203.
[21] Z. Zhang, T. Gao, X. Liu, D. Li, J. Zhao, Y. Lei, Y. Wang, Influence of sound directions on acoustic field characteristics within a rectangle-shaped sonoreactor: numerical simulation and experimental study, Ultrason. Sonochem. 42 (2018) 787–794.
[22] K. Yasuda, T.T. Nguyen, Y. Asakura, Measurement of distribution of broadband noise and sound pressures in sonochemical reactor, Ultrason. Sonochem. 43 (2018) 23–28.
[23] G.S.B. Lebon, I. Tzanakis, K. Pericleous, D. Eskin, Experimental and numerical investigation of acoustic pressure in different liquids, Ultrason. Sonochem. 42 (2018) 411–421.
[24] D. Suo, B. Govind, S. Zhang, Y. Jing, Numerical investigation of the inertial cavitation threshold under multi-frequency ultrasound, Ultrason. Sonochem. 41 (2018) 419–426.
[25] Y. Kojima, Y. Asakura, G. Sugiyama, S. Koda, The effects of acoustic flow and mechanical flow on the sonochemical efficiency in a rectangular sonochemical reactor, Ultrason. Sonochem. 17 (6) (2010) 978–984.
[26] Z. Xu, K. Yasuda, S. Koda, Numerical simulation of liquid velocity distribution in a sonochemical reactor, Ultrason. Sonochem. 20 (2013) 452–459.
[27] Z. Xu, K. Yasuda, X. Liu, Simulation of the formation and characteristics of ultrasonic fountain, Ultrason. Sonochem. 32 (2016) 241–246.
[28] S. Niazi, Hashemabadi, S. Noroozi, Numerical simulation of operational parameters and sonoreactor configurations for the highest possibility of acoustic cavitation in crude oil, Chem. Eng. Commun. 201 (10) (2014) 1340–1359.
[29] M.N. Hussain, I. Janajreh, Numerical simulation and experimental testing of novel sonochemical reactor for transesterification, Waste Biomass Valor 8 (2017) 1733–1747.
[30] Y. Tian, Z. Liu, X. Li, L. Zhang, R. Li, R. Jiang, F. Dong, The cavitation erosion of ultrasonic sonotrode during large-scale metallic casting: experiment and simulation, Ultrason. Sonochem. 43 (2018) 29–37.
[31] G. Servant, J.P. Caltagirone, A. Gérardm, J.L. Laborde, A. Hita, Numerical simulation of cavitation bubble dynamics induced by ultrasound waves in a high frequency reactor, Ultrason. Sonochem. 7 (2000) 217–227.
[32] Y. An, Nonlinear bubble dynamics of cavitation, Phys. Rev. E 5 (2012) 016305.
[33] C. Vanhille, A two-dimensional nonlinear model for the generation of stable cavitation bubbles, Ultrason. Sonochem. 31 (2016) 631–636.
[34] C. Vanhille, C. Campos-Pozuelo, Acoustic cavitation mechanism: a nonlinear model, Ultrason. Sonochem. 19 (2012) 217–220.
[35] R. Jamshidi, B. Pohl, U.A. Peuker, G. Brenner, Numerical investigation of sonochemical reactors considering the effect of inhomogeneous bubble clouds on ultrasonic wave propagation, Chem. Eng. J. 189–190 (2012) 364–375.
[36] G.L. Chahine, A. Kapahi, J.K. Choi, C.T. Hsiao, Modeling of surface cleaning by cavitation bubble dynamics, Ultrason. Sonochem. 29 (2016) 528–549.
[37] K. Yasui, A. Towata, T. Tuziuti, T. Kozuka, K. Kato, Effect of static pressure on acoustic energy radiated by cavitation bubbles in viscous liquids under ultrasound, J. Acoust. Soc. Am. 130 (5) (2011) 3233–3242.
[38] X. Guo, C. Cai, G. Xu, Y. Yang, J. Tu, P. Huang, D. Zhang, Interaction between cavitation microbubble and cell: a simulation of sonoporation using boundary element method (BEM), Ultrason. Sonochem. 39 (2017) 863–871.
[39] Y. Hou, R. Zhou, X. Long, P. Liu, Y. Fu, The design and simulation of new downhole vibration device about acoustic oil recovery technology, Petroleum 1 (2015) 257–263.
[40] H. Wang, X. Li, Y. Li, X. Geng, Simulation of phase separation with large component ratio for oil-in-water emulsion in ultrasound field, Ultrason. Sonochem. 36 (2017) 101–111.
[41] M.F. Pedrotti, M.S.P. Enders, L.S.F. Pereira, M.F. Mesko, E.M.M. Flores, C.A. Bizzi, Intensification of ultrasonic-assisted crude oil demulsification based on acoustic field distribution data, Ultrason. Sonochem. 40 (B) (2018) 53–59.
[42] T.J. Tiong, L.E. Low, H.J. Teoh, J.-K. Chin, S. Manickam, Variation in performance at different positions of an ultrasonic VialTweeter – A study based on various physical and chemical activities, Ultrason. Sonochem. 27 (1) (2015) 165–170.
[43] I. Babuska, F. Ihlenburg, T. Strouboulis, S.K. Gangaraj, A posteriori error estimation for finite element solutions of Helmholtz' equation – Part II: estimation of the pollution error, Int. J. Num. Methods Eng. I 40 (21) (1997) 3883–3900.
[44] R. Kazys, R. Sliteris, R. Rekuviene, E. Zukauskas, L. Mazeika, Ultrasonic technique for density measurement of liquids in extreme conditions, Sensors 15 (2015) 19393–19415.
[45] K. Yasui, T. Kozuka, T. Tuziuti, A. Towata, Y. Iida, J. King, P. Macey, FEM calculation of an acoustic field in a sonochemical reactor, Ultrason. Sonochem. 14 (2007) 605–614.
[46] X. Rojas, B.D. Hauer, A.J.R. MacDonald, P. Saberi, Y. Yang, J.P. Davis, Ultrasonic

Interferometer for first-sound measurements of confined liquid 4He, Phys. Rev. B 89 (2014) 9. Article ID 174508.
[47] C. Javanaud, R.R. Rahalkar, Velocity of sound in vegetable oils, Eur. J. Lipid Sci. Technol. 90 (2) (1988) 73–75.
[48] D.T. Blackstock, Cylindrical waves, Fundamentals of Physical Acoustics, Wiley, New York, 2000, pp. 386–413 Chapter 11.
[49] T.A. Mamvura, S.E. Iyuke, A.E. Paterson, Energy changes during use of high-power ultrasound on food grade surfaces, S. Afr. J. Chem. Eng. 25 (2018) 62–73.
[50] S. Niazi, S.H. Hashemabadi, M.M. Razi, CFD simulation of acoustic cavitation in a crude oil upgrading sonoreactor and prediction of collapse temperature and pressure of a cavitation bubble, Chem. Eng. Res. Design: Trans. Inst. Chem. Eng. Part A 92 (1) (2014) 166–173.
[51] W.J. Galloway, An experimental study of acoustically induced cavitation in liquids, J. Acoust. Soc. Am. 26 (1954) 849–857.
[52] M.A. Cabrera-Trujillo, L.I. Sotelo-Díaz, M.X. Quintanilla-Carvajal, Effect of amplitude and pulse in low frequency ultrasound on oil/water emulsions, Dyna 83 (199) (2016) 63–68.
[53] D.J. Collins, T. Alan, K. Helmerson, A. Neild, Surface acoustic waves for on-demand production of picoliter droplets and particle encapsulation, Lab Chip 13 (16) (2013) 3225.
[54] K.A. Ramisetty, A.B. Pandit, P.R. Gogate, Ultrasound assisted preparation of emulsion of coconut oil in water: Understanding the effect of operating parameters and comparison of reactor designs, Chem. Eng. Process. Process Intensification (2015) 70–77.
[55] J.P. Canselier, H. Delmas, A.M. Wilhelm, B. Abismaïl, Ultrasound emulsification—an overview, J. Dispersion Sci. Technol. 23 (1–3) (2002) 333–349.
[56] T.J. Mason, Ultrasound in synthetic organic chemistry, Chem. Soc. Rev. 26 (1997) 443–451.
[57] Y. Kojima, H. Imazu, K. Nishida, Physical and chemical characteristics of ultrasonically-prepared water-in-diesel fuel: effects of ultrasonic horn position and water content, Ultrason. Sonochem. 21 (2) (2014) 722–728.